

Ultraluminous X-ray sources

S. Fabrika*

Special Astrophysical Observatory, Russia

E-mail: fabrika@sao.ru

The origin of Ultraluminous X-ray Sources (ULXs) in external galaxies whose X-ray luminosities exceed those of the brightest black holes in our Galaxy by hundreds and thousands of times is mysterious. The most popular models for the ULXs involve either intermediate mass black holes (IMBHs) or stellar-mass black holes accreting at super-Eddington rates. Here we review the ULX properties. Their X-ray spectra indicate a presence of hot winds in their accretion disks supposing the supercritical accretion. In recent years, new surprising results were discovered in X-ray data, ULX-pulsars and high-velocity outflows up to $0.2c$. They are also in accordance with the super-Eddington accretion. However, the strongest evidences come from optical spectroscopy. The spectra of the ULX counterparts are very similar to that of SS433, the only known supercritical accretor in our Galaxy. The spectra are apparently of WNL type (late nitrogen Wolf-Rayet stars) or LBV (luminous blue variables) in their hot state, which are very scarce stellar objects. We find that the spectra do not originate from WNL/LBV type donors but from very hot winds from the accretion disks, which have similar physical conditions as the stellar winds from these stars. The results suggest that bona-fide ULXs must constitute a homogeneous class of objects, which most likely have supercritical accretion disks.

*Accretion Processes in Cosmic Sources – APCS2016 –
5-10 September 2016,
Saint Petersburg, Russia*

*Speaker.

1. Introduction

Ultraluminous X-ray sources (ULXs) are X-ray sources with luminosities exceeding the Eddington limit for a typical stellar-mass black hole $\sim 2 \times 10^{39}$ erg s⁻¹. Despite their importance in understanding the origin of supermassive black holes that reside in most of present galaxies, the basic nature of ULXs remains unsolved [1, 2]. The most popular models for the ULXs involve either intermediate mass black holes (IMBH, 10^3 – $10^4 M_{\odot}$) [3] with standard accretion disks or stellar-mass black holes ($\sim 10 M_{\odot}$) accreting at super-Eddington rates. The last idea has been suggested [4] because of an analogy with SS 433, the only known super-accretor in the Galaxy [5, 6]. It was proposed that SS 433 supercritical disk's funnel being observed nearly face-on will appear as extremely bright X-ray source. In ULXs a moderate beaming in the funnel is needed to produce the super-Eddington X-ray luminosities. Both scenarios, however, require a massive donor in a close binary.

In last years the community has accepted a concept of the super-Eddington accretion with stellar mass black holes. It was not only related with finding of ultraluminous X-ray pulsars [7, 8, 9], there were many new interesting discoveries. At the moment three ULX pulsars were found, it was a notable achievement. All the pulsars have their X-ray spectra harder than those average in ULXs. Many models have been suggested for the ULX-pulsars including magnetic field of different strength. However, one of the best model is probably the same geometrical beaming [10] to violate the Eddington limit.

The X-ray spectra of the ULXs often show a high-energy curvature with a downturn between ~ 4 and ~ 7 keV [11]. It was called “ultraluminous state” [12]. The curvature hints that the ULX accretion disks are not standard. Inner parts of the disks may be covered with hot outflow or optically thick corona, which Comptonizes the inner disk photons. In more detail study [13] it was suggested an empirical classification scheme of the ULXs: a singly-peaked broadened disk with a maximum to harder band (BD), and two spectral components as hard ultraluminous (HUL) and soft ultraluminous (SUL) regimes. One more class of the sources called extremely soft ultraluminous regime (ULS) [14]. In some nearby regimes the sources might jump between BD–HUL, HUL–SUL [13] or SUL–ULS [15].

Although all the previous X-ray data could not prove reliably the super-Eddington accretion, recently such evidences have been found. In several ULXs high velocity outflows have been detected in the X-ray spectra. They are blueshifted absorption lines with velocities about $0.2 c$ arising in highly ionized gas. Originally such absorption lines and edges have been predicted for ULXs in [16, 17] on the grounds of SS 433. They are common residuals which depend however on the outflow velocity. The residuals have been clearly suspected [18] in several ULXs and have been discovered in [19] (NGC1313 X-1 and NGC5408 X-1), in [20] (M101 ULX-1), and in [15] (NGC55 ULX). The blueshifted absorption lines do not depend on the spectral components, in NGC1313 X-1 the regime is HUL, in NGC5408 X-1 - SUL, in NGC55 ULX - SUL/ULS, and in M101 ULX-1 - ULS.

Most of the ULXs are associated with the star-forming regions and surrounded with nebulae of a complex shape, indicating a dynamical influence of the black hole [21, 22, 23]. In Holmberg II X-1 there was a direct detection [24, 25] of nebula surrounded the ULX with a velocity dispersion of several tens of km/sec. That may be related with jets or strong outflows.

In a case of IMBH they are not distributed throughout galaxies as it would be expected for IMBHs originating from low-metallicity Population III stars [3]. The IMBHs may be produced in a runaway merging in a core of young clusters. In this case, they should stay within the clusters. It has been found [26] that all brightest X-ray sources in Antennae galaxies are located nearby to very young stellar clusters with an age less than 5 Myrs. It was concluded that the sources were ejected in the process of formation of stellar clusters in the dynamical few-body encounters. An average velocity of the ULXs in Antennae is ~ 80 km/sec. Therefore, the majority of ULXs are massive X-ray binaries with the progenitor masses larger than $50 M_{\odot}$.

However the most obvious evidence that the ULXs are super-Eddington accretion disks came from optical spectroscopy [27]. It was found that spectra of ULXs are very similar to SS 433 [28] and LBV stars in their hot state [29] or WNLh stars [30]. All these objects have strong and dense outflows.

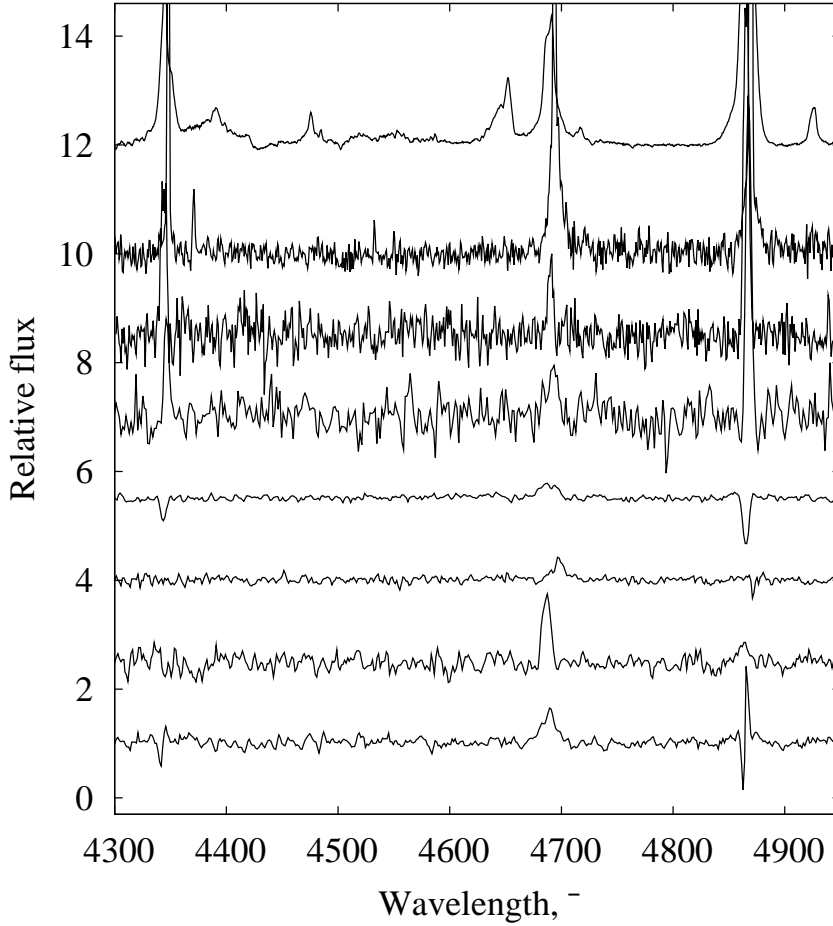


Figure 1: Normalized optical spectra of ULX counterparts. From top to bottom: SS 433 (1), NGC 5408 X-1 (2), NGC 4395 X-1 (3), NGC 1313 X-2 (2), NGC 5204 X-1 (1), NGC 4559 X-7 (1), Holmberg IX X-1 (1) and Holmberg II X-1 (1). The numbers in brackets mean optical telescopes: 1 – Subaru telescope, 2 – VLT (ESO), 3 – Russian BTA telescope. The spectra are very similar one another, they may represent rare type of massive stars WNLh [30] or LBV stars in their hot states [29]. All the spectra are also similar to SS 433 [28]. This means that the spectra of the ULX counterparts are formed in hot winds.

2. Optical spectra of ULXs

Optical spectra of almost all ULX counterparts (with SS 433 included) are shown in Fig. 1. Other spectra not shown here published in [31] (NGC7793 P13, ULX-pulsar) and in [32] (M81 ULS-1). Main features in all the spectra are the bright He II $\lambda 4686$, hydrogen H α , and H β emission lines. The lines are obviously broad, the widths range from 500 to 1500 km s $^{-1}$.

The spectra extraction was not simple due to the nebular emission that surrounds almost all the ULX counterparts. We extracted the spectra with Gauss-profile aperture, and made two versions of the spectra. In the first one, we used extended regions of 4–10 arcsec for the background. Although this gives a higher S/N in the final spectra, the hydrogen lines originating from the nebulae may strongly contaminate the ULX spectrum. In the second version, we used very small regions for the background, ≈ 1 arcsec, and produced the spectra with the least contamination by the nebular lines.

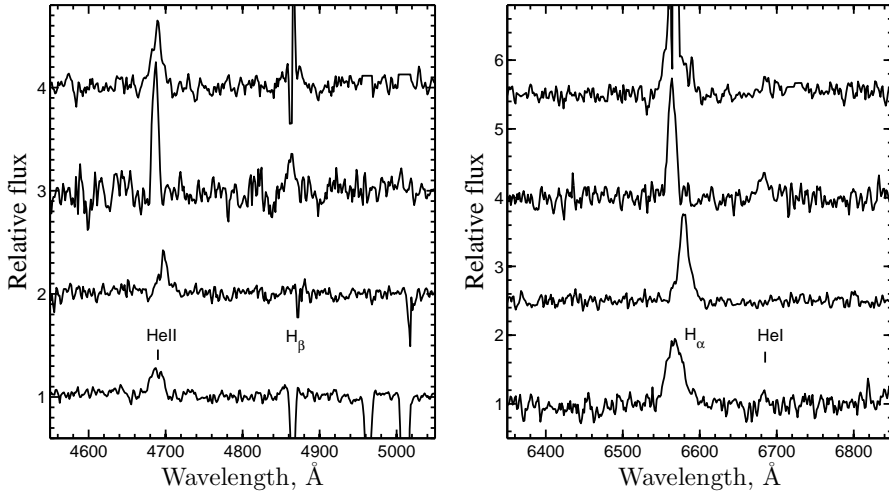


Figure 2: Spectra of the ULX optical counterparts from top to bottom, Holmberg II, Holmberg IX, NGC 4559, and NGC 5204 in blue (a) and red (b) spectral regions. The spectra are normalized for better inspection. The most strong are the He II $\lambda 4686$ line and the hydrogen lines H α $\lambda 6563$ and H β $\lambda 4861$. The broad He I $\lambda 6678$ line is also detected. Narrow nebular emission in H β and [O III] $\lambda\lambda 4959, 5007$ lines is oversubtracted. Although the hydrogen lines are contaminated with the nebular emission, their broad wings are clearly seen.

We produced the normalized spectra for better inspection of spectral features (Fig. 2) taken with the Subaru telescope [27]. The main feature in all the spectra is a broad He II $\lambda 4686$ emission line. The most narrow one is found from Holmberg IX, with an FWHM ≈ 450 km s $^{-1}$, and the most broad one is from NGC 5204, with an FWHM ≈ 1570 km s $^{-1}$. All line widths are corrected for the spectral resolution.

Calibrated spectra of the ULX optical counterparts are given in Fig. 3 (the same as in Fig. 2). We conclude that all ULX counterparts ever spectrally observed have the same feature in their spectra, that is, a broad He II emission line. We also clearly detect broad H α , H β lines and He I $\lambda\lambda 6678, 6876$ lines (Fig. 3). There is also some hints on the Bowen C III/N III blend (4640

- 4650 Å). Although the H β line (Fig. 2, 3) is affected by nebular emission in spite of our careful extraction, its broad wings are clearly detected. It is obvious that the emission lines are formed in stellar winds or disk winds.

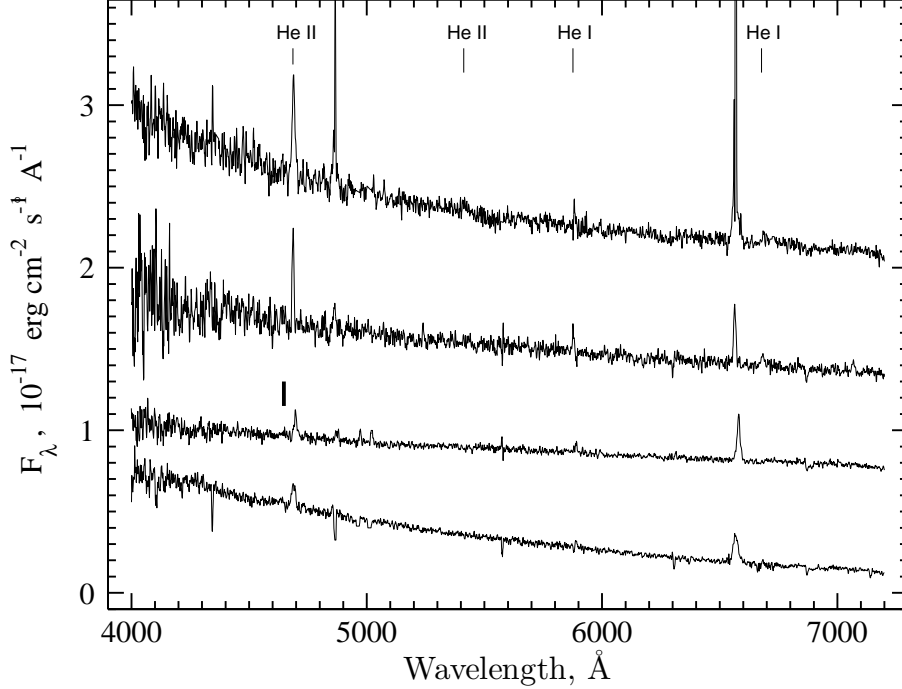


Figure 3: Calibrated spectra of the ULX optical counterparts taken with the Subaru telescope. From top to bottom: the ULX in Holmberg II, Holmberg IX, NGC 4559, and NGC 5204. For better visualization we add flux offsets of 1.8, 1.2 and 0.6 (10^{-17} erg/cm 2 s Å) for the Holmberg II, Holmberg IX, and NGC 4559 ULXs, respectively. Besides obvious hydrogen lines we mark He II lines (λ 4686 and λ 5412) and He I lines (λ 5876 and λ 6678), thick bar indicates position of the Bowen blend C III/N III λ λ 4640 – 4650.

All studied ULX have broad He II λ 4686 and H α . However, neither very hot WNLh nor LBV examples exhibit such strong He II emission lines relative to the hydrogen lines. If the abundance of hydrogen in the ULX donors were two times smaller from the Solar value, then it could make the He/H ratio five times larger. This contradicts with the non-enhancement of the He I and Pickering He II lines indicating nearly normal abundance of hydrogen. Hence, the wind in the ULXs must be even hotter and more highly ionized than stellar winds in WNLh or LBV stars.

All the spectra of the ULXs are surprisingly similar to one another. The optical spectra are also similar to that of SS 433, although the ULX spectra indicate a higher wind temperature. It was suggested in [27] that the ULXs must constitute a homogeneous class of objects, which most likely have supercritical accretion disks.

Among stellar spectra, such a strong He II line with a nearly normal hydrogen abundance can be found only in stars recently classified as O2–3.5If/WN5–7 [30]. They are the hottest transition stars, whose classification is based on the H β profile, tracing the increasing wind density (i.e., the mass loss rate) from O2–3.5If, O2–3.5If/WN5–7, and to WN5–7.

In Fig. 4 we show the classification diagram of WN stars [33] for LMC and Galactic objects.

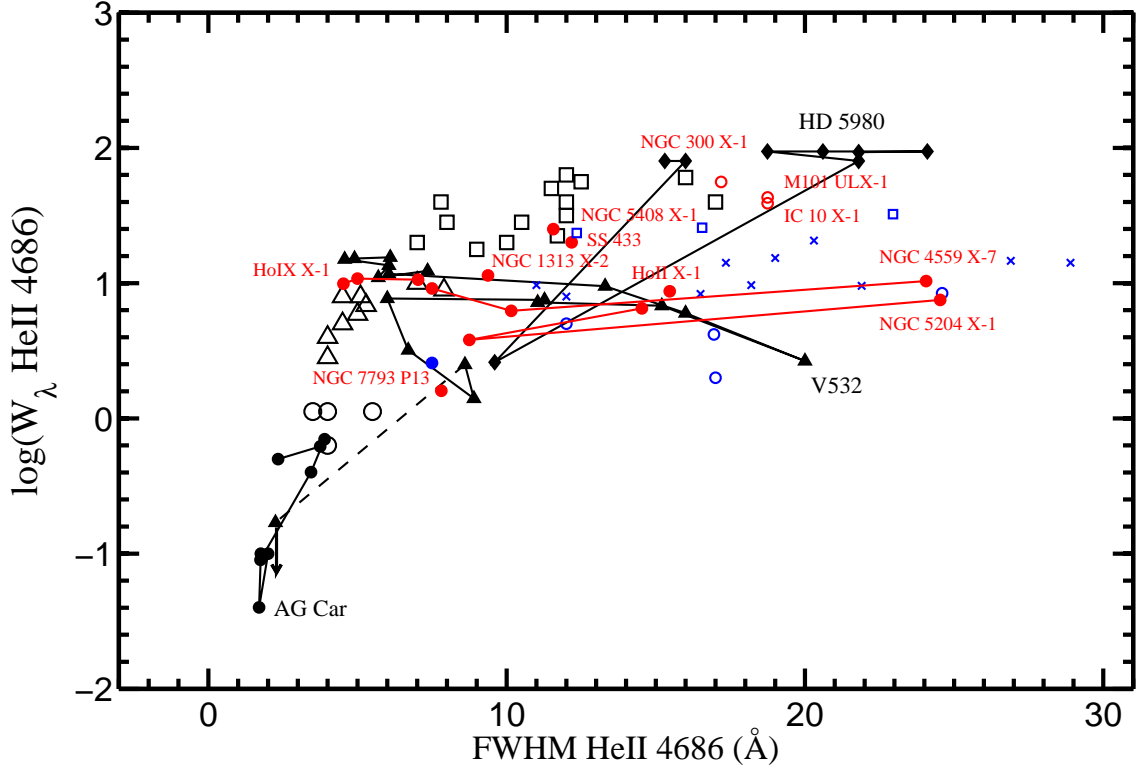


Figure 4: Classification diagram of WNL stars in the LMC and our Galaxy [33]. The black open squares, triangles, and circles mark WN 8, WN 9–10, and WN 11 stars, respectively. The blue filled circle denotes ζ Pup. Other Galactic and LMC stars [30] are O2If and O3If (open blue circles), O2If/WN5, O2.5If/WN6, O3If/WN6, and O3.5If/WN7 (blue crosses), and WN6ha and WN7ha stars (open blue squares). There are three known LBV – WNL transitions (AG Car, V 532, and HD 5980) in this diagram [29]. Consequent states of each LBV star are connected with the lines. Positions of our four ULX counterparts are also shown in red (connected with lines to show variability from night to night), together with those of NGC 1313 X-2, NGC 5408 X-1, NGC 7793 P13, SS 433, NGC 300 X-1, M 101 ULX-1, and IC 10 X-1 [34, 35, 31, 28, 36, 37, 38].

We supplement the diagram with additional stars recently classified [30]. The diagram plots stars in accordance with their wind velocity (FWHM, the terminal velocity of a stellar wind), while the equivalent width (EW) reflects its photosphere temperature and a mass loss rate. Three known LBV transitions (LBV – WNL) between their hot and cool states in AG Car, V 532 in M 33, and HD 5980 in SMC are also shown in the figure. The transitions last from months to years. Consequent states in each LBV transition are connected with the lines. In their hotter LBV-state where the He II line becomes stronger, the LBVs fit well the classical WNL stars [29].

In the figure, we also present two recently discovered extragalactic black holes NGC 300 X-1 and IC 10 X-1 together with the soft ULX transient M 101 ULX-1. The black holes in NGC 300 X-1 and IC 10 have luminosities $L_X \sim 3 \times 10^{38} \text{ erg s}^{-1}$, they contain the WN donors. About the same as that of Cyg X-3, which certainly contains a WN-type donor star [39]. The comparable luminosities with that of Cyg X-3, short orbital periods, and the location in the diagram around the WN6–7 region confirm that their optical spectra come from WN donors. The same may be proposed for

M 101 ULX-1 on the basis of its location in the diagram. It has been recently found that this source indeed contains a WN8 type donor [40], although its orbital period is ~ 40 times longer than in Cyg X-3 and ~ 6 times longer than in two other WR X-ray binaries.

Thus, the ULX counterparts and SS 433 occupy a region at this diagram between O2–3.5If and WN5–7. This is also a region of “intermediate temperature LBV” V 532 and the “LBV excursion” of HD 5980. The variability of the He II lines of our counterparts in three consequent nights is shown by the points connected by the lines. However, their behavior in the He II diagram is nothing like stars. They exhibit night-to-night variability both in the line width and equivalent width by a factor of 2–3. Variability in the radial velocity of the line is also detected with amplitudes ranging from 100 to 400 km/sec [27].

If the ULX counterpart spectra were produced from donor stars, variable surface gravity at about the same photospheric temperature would be required. Instead, the spectra may be formed in unstable and variable winds formed in accretion disks. This idea agrees with the fact that we do not find any regularities between the EW, FWHM, and radial velocity of the He II line.

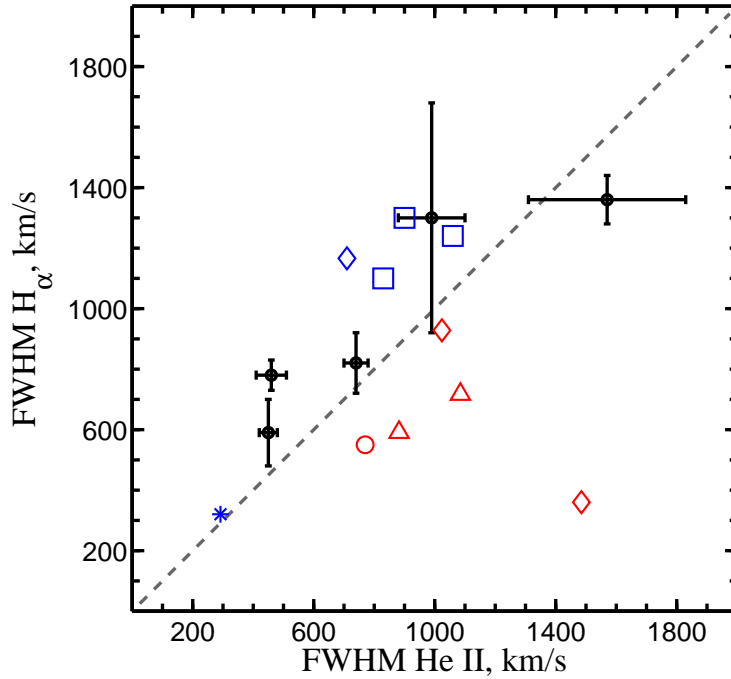


Figure 5: Emission line widths of He II and H α . The ULX counterparts with simultaneous spectra (points with error bars) are shown from top to bottom: NGC5204 X-1, Holmberg II X-1, NGC5408 X-1 (Cseh et al. 2013), NGC4559 X-7, Holmberg IX X-1. Also shown SS 433 (blue diamond) from [28, 41] taken in the same precessional phase, the LBV star V532 in M33 [29] in its hot state (asterisk), and three transitional stars (square) WR22/WN7ha, WR24/WN6ha, WR25/WN6ha [42]. The transient black hole binaries with heated accretion disks look another: GX339-4 [43, 44] (circle), V404 Cyg [45, 46] (triangle), and GRO J1655-40 [47, 48] (red diamond). The X-ray transients may look as a probable analogue of IMBH with an accretion disk.

Therefore we can exclude the case where these ULXs actually have WNL donors and their stellar winds produce the observed optical spectra. The rapid variability of the He II line-width is difficult to be explained, because the wind terminal velocity in stars is determined by the surface

gravity. Other arguments may be found in [27]. Opposite situation is in NGC 300 X-1, M 101 ULX-1, and IC 10 X-1, where the He II line is stable and has not a strong variability, this line is also shows a clear orbital solution.

A clear difference between strong outflows and heated accretion disks is shown in Fig. 5. Indeed, such emission lines from the self-irradiated disk are observed from Galactic stellar-mass black hole X-ray binaries in ourbursts, such as GRO J1655–40, V404 Cyg and GX 339–4. In these cases, the width of the He II lines is broader than hydrogen lines, as expected. We can interpret that their irradiated disks are not blocked by disk winds completely, and hence we observe both the He II and H α emissions directly at the disk surface.

By contrast, our optical spectra of the ULXs have revealed that the He II emission line is always narrower than the H α (Fig. 5) line. This fact would be very difficult to be explained by standard disks. Such a situation is observed in all hot supergiants with strong winds, WNL, LBV stars and SS 433. When the wind is accelerated, upper and farther parts of the wind are turning colder and have higher velocities. It is the best evidence that of a supercritical accretion in ULXs.

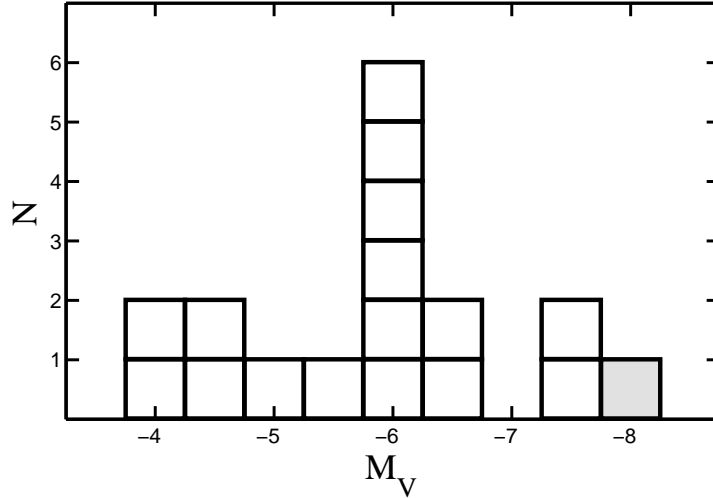


Figure 6: Absolute magnitudes of all well-studied ULXs and SS 433 (shaded). The data are from [49, 50, 51, 52].

In Fig. 6 we show absolute magnitudes of the well-studied ULXs. The ULXs have a wide distribution with a well-defined maximum at $M_V \approx -6$. In decreasing optical luminosity they are SS 433, NGC6946 ULX-1, NGC7793 P13, NGC4559 X-7, NGC5408 X-1, NGC5204 X-1, NGC4395 X-1, M81 ULS1, Holmberg II X-1, IC342 X-1, Holmberg IX X-1, NGC4559 X-10, NGC1313 X-2, NGC5474 X-1, NGC1313 X-1, M66 X-1 and M81 X-6. The faintest ULX counterparts have optical luminosities of 25–26 magnitudes, they may be objectively detected with the Hubble Space Telescope. The abrupt decrease in the number of objects with decreasing M_V probably could not be related to the effects of observational selection.

The total luminosity of a supercritical disk is proportional to the Eddington luminosity with an additional logarithmical factor depending on the original mass accretion rate [53, 54], because the excess gas is expelled as a disk wind and the accreted gas is advected with the photon trapping, contributing little to the photon luminosity. However, the UV and optical luminosity in such

disks may strongly depend on the original mass accretion rate, because these budgets are mainly produced by the reprocess of the strong irradiation from the wind (the excess gas). Therefore if the X-ray luminosity may be about the same, the optical luminosity may notably depends on the accretion rate.

It was found [27] that the mass accretion rates in the ULXs may be by a factor of 1.5–6 smaller and their wind temperatures are by 1.4–4 times higher than those in SS 433. Optical spectra of SS 433 and the ULX counterpart are nearly the same, but in X-rays they are drastically different because we cannot observe the funnel in SS 433 directly.

3. Conclusions

Why SS 433 is not strong an X-ray emitter? We observe it nearly edge-on and we could not look at its funnel [55]. We observe only the X-rays jets and the illuminating radiation coming from deeper funnel regions as reflected spectrum of the outer funnel walls [56]. In [57] have been found constraints from SS 433 funnel as a reflected signal in the Galactic plane (the molecular clouds). An upper limit was of $2 \times 10^{39} \text{ erg s}^{-1}$ in the 2-10 keV energy band.

However, SS 433 can not be a copy of ULXs because its optical luminosity is notably higher than in ULX counterparts (Fig. 6), and wind temperature is less than in ULXs. In a study of optical filaments in W 50 surrounding extended X-rays jets, He II and hydrogen lines were discovered there. It was found using the ionization thresholds of He II and H I in the filaments [58] that a funnel in SS 433 has a temperature 50 – 70 kK and its isotropic UV luminosity is $\sim 10^{40} \text{ erg s}^{-1}$. In such a case SS 433 may be close relative to ULSs [14]. In well-studied ULSs, for example M81 ULS-1 and NGC247 ULS, their optical luminosities are $M_V \approx -6.1$ and $M_V \approx -5.2$ respectively. The supercritical disk in SS 433 has a luminosity of $M_V \approx -7.8$. The optical luminosity in SS 433 is bigger than in standard ULSs.

We may conclude that the ULX/ULSs have about face-on supercritical disks, nevertheless their optical luminosities and winds are not as powerful as that in SS 433. In this sense, SS 433 remains the unique object.

Acknowledgments

The research was supported by the Russian Science Foundation grant (N 14-50-00043) and RFBR grant (N 16-02-00567).

References

- [1] H. Feng & R. Soria *New Astron. Rev.* **55**, 166 (2011)
- [2] M. Bachetti *AN* **337**, 349 (2016)
- [3] P. Madau & M.J. Rees *ApJ* **551**, L27 (2001)
- [4] S. Fabrika & A. Mescheryakov *IAUS* **205**, 268 (2001)
- [5] S. N. Fabrika *Ap&SS* **252**, 439 (1997)
- [6] S. Fabrika *ASPRv* **12**, 1 (2004)

- [7] M. Bachetti, F. A. Harrison, D. J. Walton, et al. *Nature* **514**, 202 (2014)
- [8] F. Fürst, D. J. Walton, D. Stern, et al. *ApJ* **834**, 77 (2017)
- [9] G. L. Israel, A. Papitto, P. Esposito, L. Stella, et al. *MNRAS* **466**, L48 (2017)
- [10] T. Kawashima, S. Mineshige, K. Ohsuga & T. Ogawa *PASJ* **68**, 83 (2016)
- [11] A.-M. Stobbart, T. P. Roberts & J. Wilms *MNRAS* **368**, 397 (2006)
- [12] J. C. Gladstone, T. P. Roberts & C. Done *MNRAS* **397**, 1836 (2009)
- [13] A. D. Sutton, T. P. Roberts & M. J. Middleton *MNRAS* **435**, 1758 (2013)
- [14] R. Urquhart & R. Soria *MNRAS* **456**, 1859 (2016)
- [15] C. Pinto, W. Alston, R. Soria, et al. *arXiv:1612.05569* (2016)
- [16] S. Fabrika, S. Karpov, P. Abolmasov & O. Sholukhova *IAUS* **230**, 278 (2006)
- [17] S. N. Fabrika, P. K. Abolmasov & S. Karpov *IAUS* **238**, 225 (2007)
- [18] M. J. Middleton, D. J. Walton, A. Fabian et al. *MNRAS* **454**, 3134 (2015)
- [19] C. Pinto, M. J. Middleton & A. C. Fabian *Nature* **533**, 64 (2016)
- [20] R. Soria & A. Kong *MNRAS* **456**, 1837 (2016)
- [21] P. Abolmasov, S. Fabrika, O. Sholukhova & V. Afanasiev *Astrophys. Bull.* **62**, 36 (2007)
- [22] F. Grisé, P. Kaaret, S. Corbel, et al. *ApJ* **745**, 123 (2012)
- [23] D. Cseh, S. Corbel, P. Kaaret, et al. *ApJ* **749**, 17 (2012)
- [24] I. Lehmann, T. Becker, S. Fabrika, et al. *A&A* **431**, 847 (2005)
- [25] O. V. Egorov, T. A. Lozinskaya & A. V. Moiseev *MNRAS* **467**, L1 (2017)
- [26] J. Poutanen, S. Fabrika, A. Valeev, et al. *MNRAS* **432**, 506 (2013)
- [27] S. Fabrika, Y. Ueda, F. Vinokurov, O. Sholukhova & M. Shidatsu *Nat. Phys.* **11**, 551 (2015).
- [28] K. Kubota, Y. Ueda, S. Fabrika, et al. *ApJ* **709**, 1376 (2011)
- [29] O. N. Sholukhova, S. N. Fabrika, A. V. Zharova, et al. *Astrophys. Bull.* **66**, 123 (2011)
- [30] P. A. Crowther & N.R. Walborn *MNRAS* **416**, 1311 (2011)
- [31] C. Motch, M. W. Pakull, R. Soria, et al. *Nature* **514**, 198 (2014)
- [32] J.-F. Liu, Y. Bai, S. Wang, S. Justham, et al. *Nature* **528**, 108 (2015)
- [33] P. A. Crowther & L. J. Smith *A&A* **320**, 500 (1997)
- [34] T. P. Roberts, J. C. Gladstone, A. D. Goulding, et al. *AN* **332**, 398 (2011)
- [35] D. Cseh, F. Grisé, S. Corbel & P. Kaaret *ApJ* **728**, L5 (2011)
- [36] P. A. Crowther, R. Barnard, S. Carpano, et al. *MNRAS* **403**, L41 (2010)
- [37] K. D. Kuntz, R. A. Gruendl, Y.-H. Chu, et al. *ApJ* **620**, L31 (2005)
- [38] J. M. Silverman & A. V. Filippenko *ApJ* **678**, L17 (2008)
- [39] M. H. van Kerkwijk, T. R. Geballe, D. L. King, et al. *A&A* **314**, 521 (1996)
- [40] J.-F. Liu, J. N. Bregman, Y. Bai, et al. *Nature* **503**, 500 (2013)

- [41] S. A. Grandi & R. P. S. Stone *PASP* **94**, 80 (1982)
- [42] N. R. Walborn & E. L. Fitzpatrick *PASP* **112**, 50 (2000)
- [43] R. Soria, K. Wu & H. M. Johnston *MNRAS* **310**, 71 (1999)
- [44] F. Rahoui, M. Coriat & J. C Lee *MNRAS* **442**, 1620 (2014)
- [45] J. Casares, P. A. Charles, D. H. P. Jones, et al. *MNRAS* **250**, 712 (1991)
- [46] E. Gotthelf, J. P. Halpern, J. Patterson & R. M. Rich *AJ* **103**, 219 (1992)
- [47] R. W. Hunstead, K. Wu & D. Campbell-Wilson *ASPC* **121**, 63 (1997)
- [48] R. Soria, D. T. Wickramasinghe, R. W. Hunstead & K. Wu *ApJ* **495**, L95 (1998)
- [49] L. Tao, H. Feng, F. Grisé & P. Kaaret *ApJ* **737**, 81 (2011)
- [50] A. Vinokurov, S. Fabrika & K. Atapin *Astrophys. Bull.* **68**, 139 (2013)
- [51] S. Avdan, A. Vinokurov, S. Fabrika, et al. *MNRAS* **455**, L91 (2016)
- [52] A. Vinokurov, S. Fabrika & K. Atapin *arXiv:1606.03024* (2016)
- [53] N. I. Shakura & R. A. Sunyaev *A&A* **24**, 337 (1973)
- [54] J. Poutanen, G. Lipunova, S. Fabrika, et al. *MNRAS* **377**, 1187 (2007)
- [55] E. Filippova, M. Revnivtsev, S. Fabrika, et al. *A&A* **460**, 125 (2006)
- [56] A. Medvedev S. & Fabrika *MNRAS* **402**, 479 (2010)
- [57] I. Khabibullin & S. Sazonov *MNRAS* **457**, 3963 (2016)
- [58] S. N. Fabrika & Sholukhova *Proceedings of the VII Microquasar Workshop: Microquasars and Beyond* p. 52 (2008)